



Activated carbon supported iron-nickel bimetallic nanoparticles for decolorization of Reactive Black 5 wastewater

Hung-Yee Shu*, Ming-Chin Chang, Hsin-Wen Hsu

Institute of Environmental Engineering, Hungkuang University, Taichung 433, Taiwan, Tel. +886 426318652, ex. 1200 (H.-Y. Shu), ex. 4113 (M.-C. Chang), ex. 4123 (H.-W. Hsu); emails: hyshu@sunrise.hk.edu.tw (H.-Y. Shu), chang@sunrise.hk.edu.tw (M.-C. Chang), hdagf1204@yahoo.com.tw (H.-W. Hsu)

Received 15 January 2014; Accepted 19 June 2014

ABSTRACT

In this study, a synthesized activated carbon supported iron-nickel bimetallic nanoparticles complex (nFeNi-GAC) material was proposed for the decolorization of wastewater which contained Reactive Black 5. From results, the successful reductive decolorization of RB5 wastewater was observed using nFeNi-GAC material. An nFeNi-GAC load of 20 g l^{-1} with various Fe/Ni compositions was capable to decolorize RB5 from 80 to 100%. For fixed Fe/Ni ratio of 6.91:0.86, the higher nFeNi-GAC dosage performed, the higher RB5 removal efficiency. At very high initial RB5 concentration of 800 mg l^{-1} , 20 g l^{-1} nFeNi-GAC material was able to remove about 80% of RB5 dye. The nFeNi-GAC material showed excellent pH resistant ability than nano iron-nickel bimetallic particles without support. For temperature from 0 to 60°C , the reductive decolorization rate increased with increasing temperature. From durability test, for three cycles of reductive decolorization, nFeNi-GAC material still showed about 96% of decolorization efficiency. Consequently, the nFeNi-GAC material performed effectively for decolorization of RB5 wastewater, offering great potential in application in azo dye wastewater treatment application.

Keywords: Nanoparticle; Iron-nickel bimetallic particles; Activated carbon; Decolorization; Azo dye

1. Introduction

Textile industry with over 250 textile dyeing and processing factories is one of the most important industries in Taiwan. From governmental statistics, the textile industry contributed 11,820 million US dollars export revenue which was about 3.9% total export revenue in year 2012 [1]. Due to more restricted regu-

lation, textile dyeing and processing factories are forced to develop and conduct more efficient pre-treatment or polishing processes for the decolorization of this type of high color and high chemical oxidation demand wastewater. Therefore, treatment technologies dealing with effluents from dyeing related industries draw much attention from research communities and industries, recently [2–4]. Among dyestuff materials used in textile industry, azo dyes are the largest

*Corresponding author.

Presented at the 6th International Conference on the "Challenges in Environmental Science and Engineering" (CESE-2013), 29 October–2 November 2013, Daegu, Korea

category of commercial dyes. Therefore, many studies reported their efforts on investigating various technologies for decomposition of azo dye compounds [5–7]. The di-azo dye used in this study, C.I. Reactive Black 5, was utilized extensively in various textile dyeing industries.

Initiating from reactive barrel for soil and ground-water remediation, zero-valent iron was introduced to the environmental applications. Thereafter, according to the dynamical development of innovative nanotechnology, nano scale zero-valent iron, i.e. NZVI, technology has been applied in environmental technologies. Successful applications of NZVI and bimetallic nanoparticles for dechlorination of chlorinated hydrocarbons such as TCE, polychlorinated biphenyls, and chlorinated ethanes [8–10] in remediation of contaminated soil and groundwater were reported. Inorganic contaminants such as nitrate, perchlorate, and heavy metals were also demonstrated to be remedied by NZVI [11–13]. In spite of successful performance in soil and groundwater cases, the use of NZVI for treating azo dyes in wastewater was also demonstrated by researchers. Chang et al. presented the efficient decolorization of an Acid Black 24 azo dye by ZVI under ambient condition [14]. Furthermore, the use of NZVI with higher surface area and reactivity for Acid Black 24 wastewater treatment was reported to spend only about 6/1,000 dosage in comparison with micro scale ZVI [15].

Large specific surface area and surface reactivity make NZVI powerful for degradation organic pollutants. However, the nano scale size of NZVI makes it hard to be collected after reaction. This property causes the release or escape of nano particles into the environment which may develop the nano toxicity to human or animals. Furthermore, to build effective collecting equipment for NZVI may increase capital and operational cost. Therefore, immobilizing NZVI particles on supporting materials does not only provide an easy operation but also maintain the excellent reduction ability of NZVI. From previous researches, Li et al. utilized innovative NZVI supported on resin for effective debromination of brominated diphenyl ether [16], Shu et al. presented successful decolorization of Acid Blue 113 by NZVI immobilizing ion exchange resin [17]. Thus, cation exchange resin has been proven to be an excellent carrier for nano particles. On the other hand, granular activated carbon (GAC) with large specific surface area is also a very excellent carrier to support catalysts. This makes GAC an alternative choice for NZVI immobilization.

In this study, the reductive decolorization of azo dye C.I. Reactive Black 5 (RB5) using an activated carbon supported nano iron nickel bimetallic complex

material (nFeNi-GAC) was investigated. Operating parameters such as iron/nickel composition, nFeNi-GAC dosage, initial dye concentration, pH, and temperature were investigated.

2. Materials and methods

2.1. Materials and apparatus

A dis-azo dye, C.I. Reactive Black 5 (RB5) was selected as target compound for this reductive decolorization study. RB5 ($C_{26}H_{21}N_5Na_4O_{19}S_6$, characterized wavelength at 599 nm, molecular weight of $991.82 \text{ g mol}^{-1}$, 55% purity) was purchased from Sigma-Aldrich, Inc. and used as received without further purification. The chemical structure of RB5 is shown in Fig. 1. Commercially available Calgon F400 GAC was purchased from Calgon Inc. for preparing the GAC supported nano iron-nickel bimetallic complex material (nFeNi-GAC). Chemicals in reagent grade such as iron chloride ($FeCl_3$), nickel chloride ($NiCl_2$), and sodium borohydride ($NaBH_4$) were all purchased from Merck & Co. Inc.

The activated carbon supported nano iron-nickel bimetallic complex material (nFeNi-GAC) was prepared by initially weighing 20.0 g of Calgon F400 GAC and storing it in a 250 ml width-mouth plastic bottle. The GAC was mixed with 200 ml of iron chloride and nickel chloride binary solution and shaken at 100 rpm for 24 h to homogeneously obtain ferric ion (Fe^{3+}) and nickel ion (Ni^{2+}) adsorption in the GAC. Moreover, the ferric and nickel adsorbed GAC was washed by de-ionized (DI) water three times to remove residual $FeCl_3$ and $NiCl_2$ from GAC. Later, 0.8 M of $NaBH_4$ solution was added to obtain nano iron and nickel precipitation in the GAC at an ambient temperature to form nFeNi-GAC following

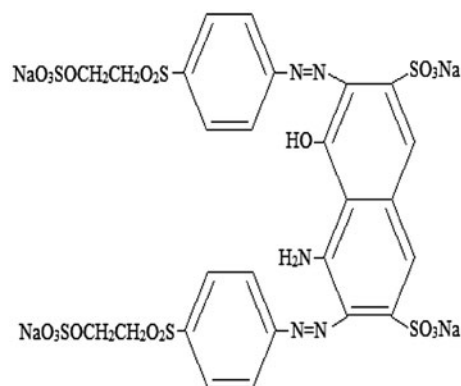
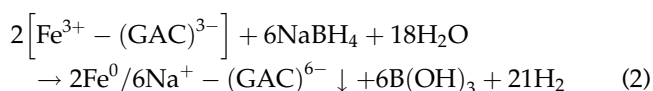
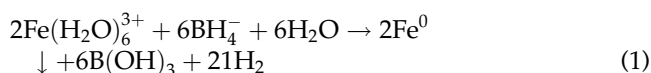


Fig. 1. The chemical structure of target compound C.I. Reactive Black 5.

Eqs. (1) and (2) (showed only for NZVI formation). The above method was modified from a previous study [17]. Afterwards, DI water was used to wash the nFeNi-GAC three times and remove residual NaBH₄ solution. A partial amount of the nFeNi-GAC was taken to identify the morphology by a JEOL 6330CF Field Emission Scanning Electron Microscope (FESEM). The morphology image of bare GAC is shown in Fig. 2(a) and the nFeNi-GAC shown in Fig. 2(b). And the 10,000 times enlargement image of bare GAC and nFeNi-GAC are shown in Fig. 2(c) and (d), respectively. In this way, the particle sizes of nano iron-nickel bimetallic particles were observed to be less than 100 nm from of FESEM image. Furthermore, the iron and nickel loads on GAC was measured by microwave digestion of nFeNi-GAC sample and analyzed by a SHIMADZU AA-6200 Atomic Absorption Spectroscopy.



2.2. Experimental procedure and analysis

The nFeNi-GAC was initially prepared by 20 g Calgon F400 GAC in a 200 ml various concentration compositions of iron chloride and nickel chloride binary solution to obtain various nano iron and nickel loadings. 20 g of nFeNi-GAC was placed in the 11 batch reactor. The amount (in mg unit) of dye RB5 was precisely measured to dissolve into 11 of DI water, obtaining a concentration of mg l⁻¹ unit. The RB5 dye solution was poured into the reactor, taking into consideration the time, loading of nFeNi-GAC, initial dye concentration, pH, and temperature at mixing rate of 150 rpm. The reaction runs were performed at ambient temperature of 25 ± 1 °C and unadjusted solution pH of 6.0 ± 0.3 in all cases not investigating effects of temperature and pH. At defined time

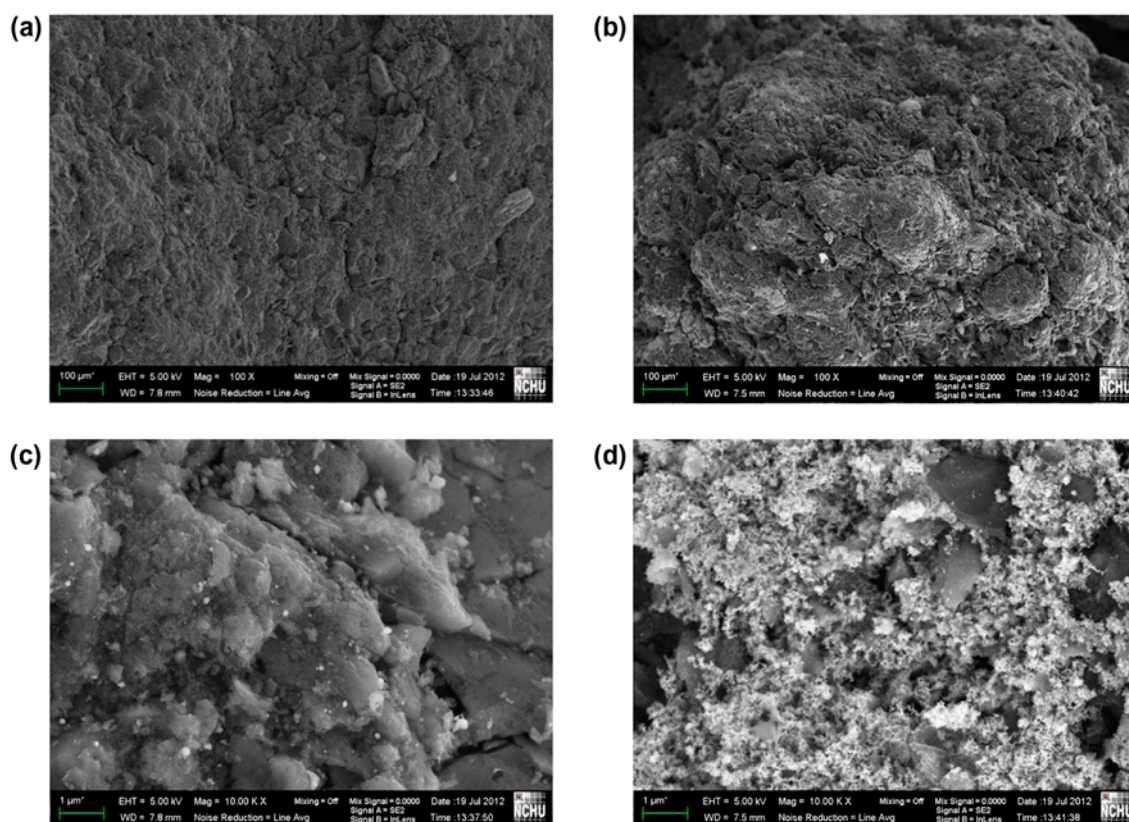


Fig. 2. FESEM images for (a) bare GAC and (b) nFeNi-GAC at 100 times enlargement, and (c) bare GAC, (d) nFeNi-GAC at 10,000 times enlargement (the nFeNi-GAC Fe/Ni composition of 6.91 mg Fe/0.86 mg Ni g⁻¹).

intervals, the dye concentration in water samples were withdrawn and measured by a Hitachi U-2000 spectrophotometer with single wavelength absorbance (599 nm) duplicated. The total organic carbon was determined by an IO Analytical 1030W Total Organic Carbon analyzer. The standard color detection procedure developed by the American Dye Manufacturers Institute (ADMI) was employed to evaluate the color intensity of RB5 dye solution. The color intensity was calculated by applying the Adams–Nickerson color difference formula, which substituted transmittance data obtained into 30 wavelengths from 400 to 700 nm in every 10 nm interval, following method 2120E of the Standard Methods. The pH and oxidation reduction potential (ORP) were monitored by a Eutech PH5500 dual channel pH/ion meter with specific probes. The iron and nickel concentrations were measured by a Shimadzu AA-6200 Atomic Absorption Spectrophotometer. Several sets of calibration curves were prepared under various pH conditions (i.e. pH 2, 3, 6, 9, and 11) to reflect the variation of characteristic wavelength and absorbance. And these calibration curves were used to measure the RB5 concentrations under various pH conditions to avoid expected error. In order to test the durability of nFeNi-GAC material, nFeNi-GAC after designed decolorization experiment was separated from reaction solution by filtration and washed three times by DI water. Then this recovered nFeNi-GAC material was then applied to a new set of decolorization experiment. The performance of this recovered nFeNi-GAC was used to evaluate the durability of nFeNi-GAC complex material.

3. Results and discussion

3.1. Effect of iron/nickel composition

The mechanism of reductive decolorization by NZVI was reported in our previous study which proposed the cleavage of azo link on the azo dye molecule is the main reason of decolorization [15]. Similar reductive decolorization behavior was also presented for resin supported NZVI [17]. With advantage of large specific surface area, GAC in this work played an excellent carrier role to support NZVI. As a superb adsorption material, GAC is able to remove RB5 azo dye by adsorption mechanism. In order to verify the contributions of adsorption and reductive decolorization by nFeNi-GAC in our designed system, a set of control experiments using NZVI, GAC, and nFeNi-GAC for decolorizing RB5 solution were performed. Fig. 3(a) shows the effect of reaction time on the removal of RB5 dye under NZVI reduction, GAC adsorption, and nFeNi-GAC reaction with the addition

of 90 mg l⁻¹ NZVI with 40 mg l⁻¹ Ni, 20 g l⁻¹ GAC, and 20 g l⁻¹ of 6.91 mg Fe/0.86 mg Ni g⁻¹ nFeNi-GAC, respectively, for initial dye concentration of 50 mg l⁻¹. For NZVI reduction decolorization, within the first 2 min, the removal of RB5 concentration was about 51%, increasing sharply up to 91% in 10 min. The pseudo-first-order rate constant was obtained to be 0.331 min⁻¹ ($R^2=0.992$) by curve fitting. For GAC adsorption, the removal of RB5 was rather slower than NZVI reduction decolorization. It reached 29% removal for first 10 min. The pseudo-first-order rate constant was calculated to be 0.026 min⁻¹ ($R^2=0.989$), it was less than 1/10 of NZVI rate constant. The pseudo-first-order rate expression of NZVI reduction decolorization and GAC adsorption of RB5 were as follows,

$$\text{RB5 } R\% (\text{NZVI}) = 1 - e^{-k_1 t} \quad (3)$$

$$\text{RB5 } R\% (\text{GAC}) = 1 - e^{-k_2 t} \quad (4)$$

where, RB5 $R\%$ denotes the removal efficiency of RB5 under NZVI reduction or GAC adsorption removal of RB5. The constants k_1 and k_2 (min⁻¹) denote the pseudo-first-order rate constants of NZVI reduction and GAC adsorption of RB5, respectively.

For nFeNi-GAC reaction, the system was influenced by both NZVI reduction and GAC adsorption. Therefore, the pseudo-first-order reaction equation can be modified as follows,

$$\text{RB5 } R\% = A \times (1 - e^{-k_1 t}) + B \times (1 - e^{-k_2 t}) \quad (5)$$

where RB5 $R\%$ denotes the removal efficiency of RB5 under nFeNi-GAC reaction. A presents the contribution percentage of NZVI on RB5 removal. B is the contribution percentage of GAC adsorption on RB5 removal. Furthermore, k_1 and k_2 (min⁻¹) are same definition as for Eqs. (3) and (4).

Modeling by curve fitting, the pseudo-first-order rate constants were obtained for NZVI reduction and GAC adsorption to be 0.383 and 0.043 min⁻¹, respectively. The contribution of NZVI reduction and GAC adsorption were calculated to be 77.1 and 19.5%, respectively. The results suggest that NZVI reduction is the major mechanism of RB5 decolorization in nFeNi-GAC reaction system for its exactly higher reaction rate and heavier contribution to the RB5 removal.

The ORP of a solution is a measure of the oxidizing or reduction power of the solution. In an oxidizing environment with presence of an oxidizing agent, a

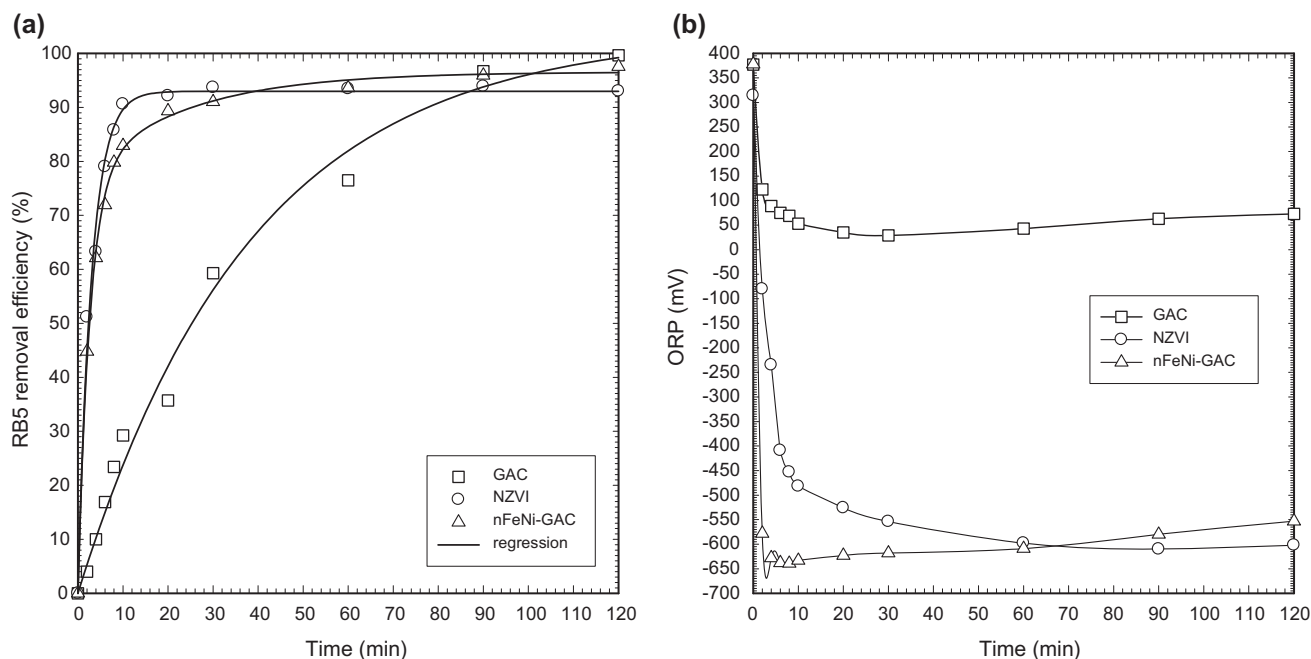


Fig. 3. Comparisons of GAC adsorption, NZVI reduction, and nFeNi-GAC reaction on (a) RB5 removal efficiency and (b) ORP. The operation conditions were initial dye concentration of 50 mg l^{-1} , GAC load of 20 g l^{-1} , NZVI dosage of 90 mg l^{-1} NZVI with 40 mg l^{-1} Ni, Fe/Ni load on nFeNi-GAC of $6.91 \text{ mg Fe}/0.86 \text{ mg Ni g}^{-1}$, nFeNi-GAC dosage of 20 g l^{-1} and reaction time during 120 min.

higher ORP with positive value will exist. On the other hand, a lower ORP presents a more reducing environment. From results of Fig. 3(b), in GAC adsorption experiment, the highest ORP was measured to be 377 mV and slowly dropped down to about 30 mV . During whole reaction process, the ORP maintained positive values to show an oxidizing environment. For both NZVI reduction and nFeNi-GAC reaction experiments, the highest ORPs were measured as 314 and 378 mV , respectively, at the beginning of the reaction. Then the ORPs of NZVI reduction and nFeNi-GAC reaction dropped sharply down to -633 and -482 mV in 10 min, respectively. For whole experiment, the ORPs kept large negative values to present reductive environment.

The effect of the iron/nickel composition on RB5 degradation shown in Fig. 4(a) indicates that RB5 degradation efficiency increases with the increase of the iron composition on nFeNi-GAC at higher iron dosage over 4.53 mg g^{-1} . Thus, the RB5 removal efficiency is the function of the Fe/Ni binary composition (i.e. $3.82\text{--}7.53 \text{ mg Fe g}^{-1}$ with $0.24\text{--}4.92 \text{ mg Ni g}^{-1}$) and reaction time by 20 g l^{-1} nFeNi-GAC with an initial RB5 concentration of 50 mg l^{-1} . Increasing the composition of Fe to $7.53 \text{ mg Fe}/0.24 \text{ mg Ni}$ per gram of nFeNi-GAC presented highest RB5 removal efficiency. In this case, nFeNi-GAC provided substantially more

active surface sites to accelerate the initial reaction, resulting in more nano iron-nickel bimetallic surface collision with more azo dye molecules to enhance RB5 degradation.

From the experimental data, the degradation efficiencies of 11.6, 86.1, and 91.4% were obtained by the Fe/Ni compositions of $4.53/1.91$, $3.82/4.92$, and $7.53/0.24 \text{ mg g}^{-1}$ over 20 min, respectively. Moreover, the degradation efficiencies of RB5 were found to be influenced by Fe/Ni compositions. The presence of Ni on nFeNi-GAC is able to protect nano iron particles from oxidation reaction by dissolved oxygen. And existence of nano iron particles is able to provide high reductive degradation ability. From results, the nFeNi-GAC with Fe/Ni compositions of $6.91/0.86$ and $7.53/0.24$ perform fairly good RB5 degradation efficiencies at same level. Therefore, a $6.91 \text{ mg Fe}/0.86 \text{ mg Ni g}^{-1}$ composition was chosen for the rest of the experiments. GAC without iron-nickel bimetallic nanoparticles was also tested for adsorption of RB5 (showed in Fig. 3(a)). It is easy to recognize the differences between reductive degradation and adsorption removal of RB5 by nFeNi-GAC and GAC, respectively. The initial rate of reductive degradation is very fast and adsorption removal is much slower. On the other hand, the ADMI color index covered whole absorbance region is quite concerned by government and industries. In Fig. 4(b), the

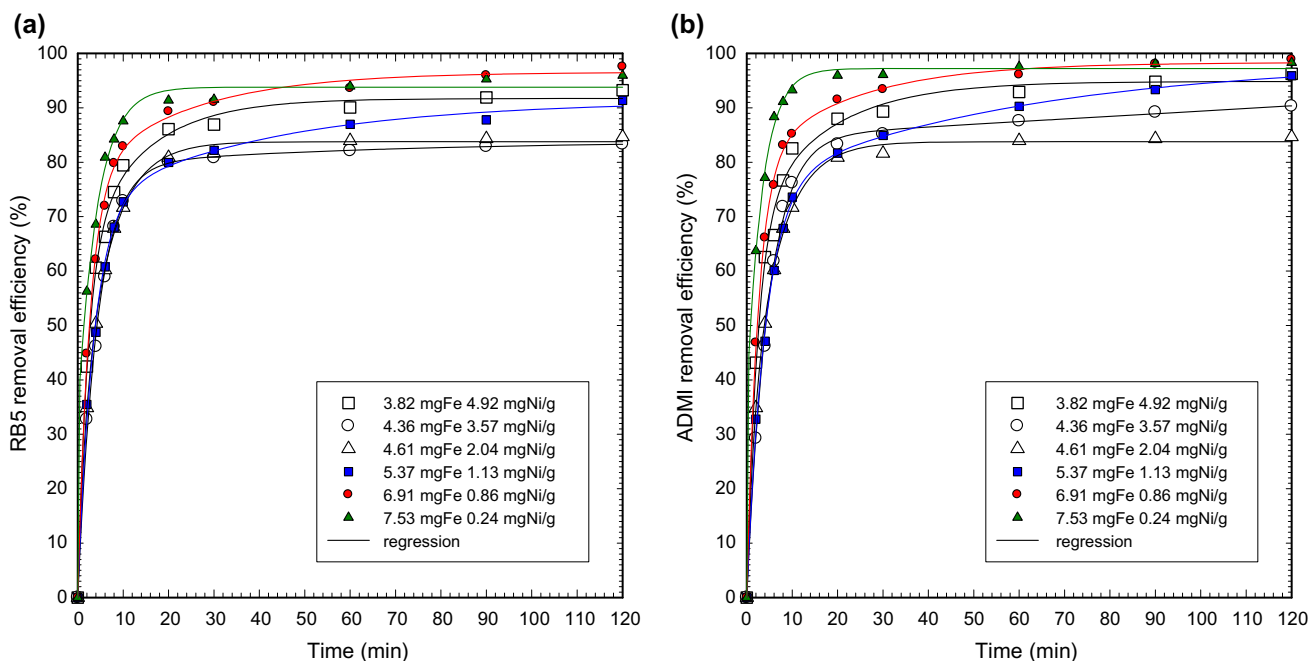


Fig. 4. Fe/Ni composition effect on (a) RB5 removal efficiency and (b) ADMI removal efficiency. The operation conditions were initial dye concentration of 50 mg l^{-1} , nFeNi-GAC dosage of 20 g l^{-1} , and reaction time during 120 min.

removal efficiencies of ADMI color for various Fe/Ni compositions were demonstrated to be similar trend with RB5 degradation.

3.2. Effect of nFeNi-GAC dosage

As shown in previous studies, the dissolution of ferrous ions and electrons to react with organic molecules on the iron surface and reduction by zero-valent iron in the aqueous phase has been proven to be a fairly fast process [14]. The performance of nFeNi-GAC follows a mechanism similar to iron dissolution, with the re-capture of free ferrous and nickel ions on the GAC surface to avoid total iron and nickel release. Fig. 5(a) shows the effect of reaction time on the degradation of RB5 dye with the addition of $10\text{--}30 \text{ g l}^{-1}$ of $6.91 \text{ mg Fe}/0.86 \text{ mg Ni g}^{-1}$ nFeNi-GAC for initial dye concentration of 50 mg l^{-1} . Within the first 2 min, the removal of RB5 concentration was about 50–75%, increasing sharply up to 10 min for higher dosage from 20 to 30 g l^{-1} . For highest dosage of 30 g l^{-1} , the RB5 dye concentration quickly dropped down to 4.3 mg l^{-1} and achieved 91.6% removal efficiency during 10 min with the initial concentration of 50 mg l^{-1} . Moreover, no significant change was found until 60 min. This scenario implies that the reductive degradation of RB5 occurs initially within the first 10 min. Afterwards, the RB5 concentration removal rarely

changes. From the results, pH increased sharply from 6.3 to 10.3 in 2 min and then kept unchanged (data not showed). The explanation of pH change in 2 min is according to the mechanism of nano iron-nickel dissolution into metal ions, spontaneously the hydroxyl ions are released into the solution and cause the increase of pH from 6.3 to 10.3. For the initial dye concentration of 50 mg l^{-1} , the ORP dropped from 437 to -629 mV as soon as the nFeNi-GAC was added. The ORP remained at about -660 mV for whole reaction period. This shows that the typical reductive condition of the RB5 dye solution was reduced within the first 10 min. After 60 min, little effective dye degradation can be found. Similarly, in Fig. 5(b) the ADMI color index decreased sharply from 9,980 down to less than 110 units during the reaction.

3.3. Effect of initial dye concentration

Fig. 6 summarizes the effect of the initial dye concentration on RB5 degradation efficiency. The maximum removal efficiency (R_{max}) declined from 97.5 to 84.9% when initial dye concentration increased from 50 to 800 mg l^{-1} . However, nFeNi-GAC presented a very good reductive degradation capability on RB5 even with extremely high concentration of 800 mg l^{-1} . This set of experiments ensures that the nFeNi-GAC is an excellent nano particle complex for decolorization

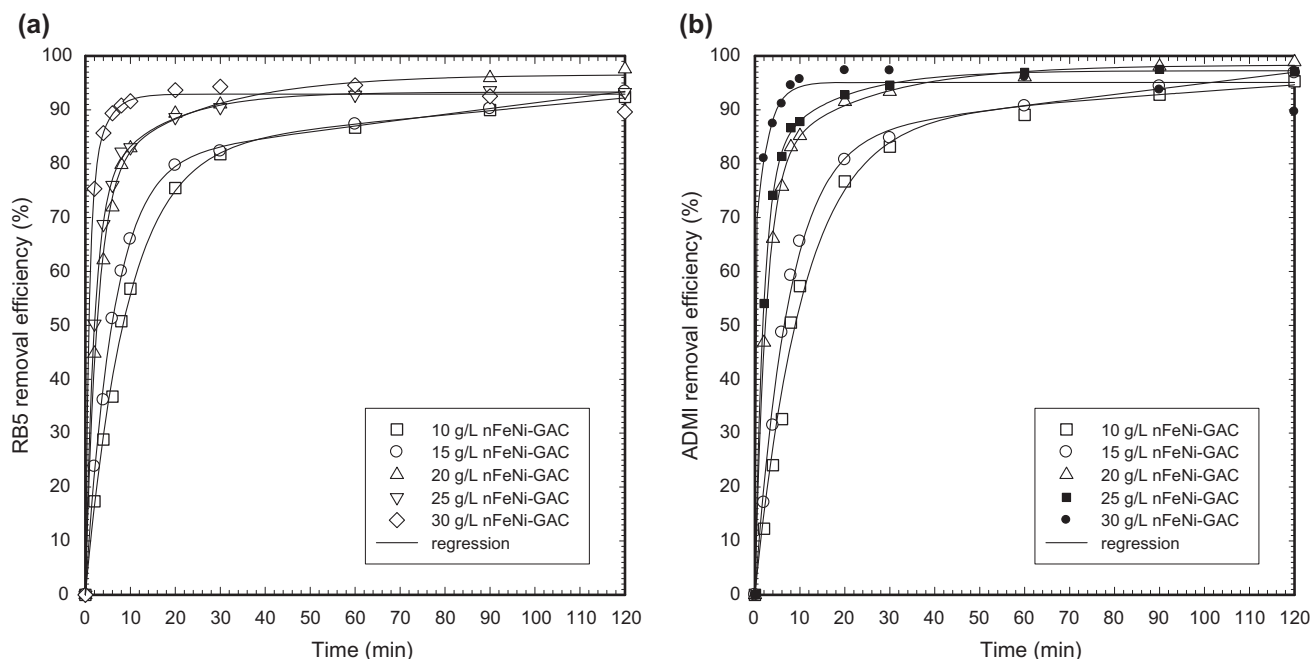


Fig. 5. Effect of nFeNi-GAC dosage on (a) RB5 removal and (b) ADMI removal. The conditions were initial dye concentration of 50 mg l^{-1} , Fe/Ni load on nFeNi-GAC of $6.91 \text{ mg Fe}/0.86 \text{ mg Ni g}^{-1}$, nFeNi-GAC dosage of $10\text{--}30 \text{ g l}^{-1}$, and reaction time during 120 min.

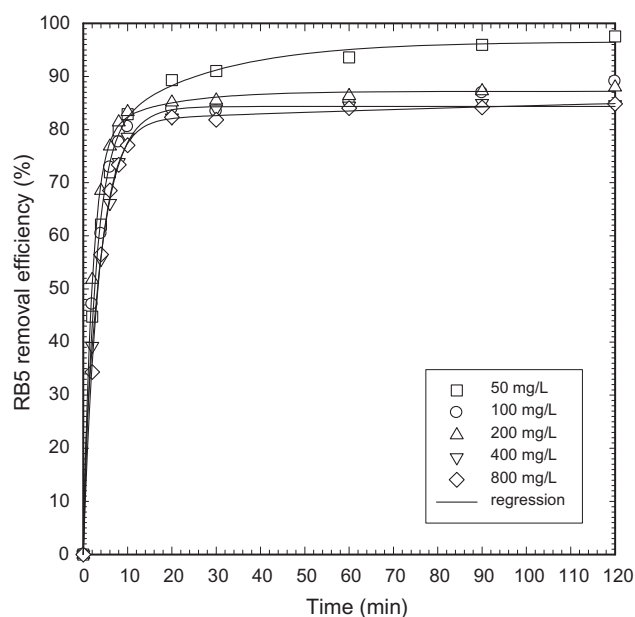


Fig. 6. Effect of initial dye concentration on RB5 degradation. The conditions were initial dye concentration of $50\text{--}800 \text{ mg l}^{-1}$, Fe/Ni load on nFeNi-GAC of $6.91 \text{ mg Fe}/0.86 \text{ mg Ni g}^{-1}$, nFeNi-GAC dosage of 20 g l^{-1} , and reaction time during 120 min.

of azo dyes. Furthermore, the initial rate (r_0) used to evaluate the effect of the initial dye concentration

increased from 11.5 to 21.5 and $133.3 \text{ mg l}^{-1} \text{ min}^{-1}$, with initial RB5 concentration increasing from 50 to 100 and 800 mg l^{-1} , respectively.

The figure shows that the unit nFeNi-GAC RB5 removal capacity (URC) is the function of the initial RB5 concentration ($50\text{--}800 \text{ mg l}^{-1}$). Over the course of 60 min, the URCs were 2.50 , 4.07 , 16.96 , and $32.92 \text{ mg RB5 per g nFeNi-GAC}$ with initial dye concentrations of 50 , 100 , 400 , and 800 mg l^{-1} by addition of 20 g l^{-1} of nFeNi-GAC. However, higher initial concentrations of RB5 obtained lower dye degradation efficiencies, which provided higher URC at the same nFeNi-GAC dosage. Thus, higher initial dye RB5 concentration showed higher URC.

3.4. Effect of pH

In our previous study, negative effects of reductive decolorization by acidic and alkaline pH were observed for NZVI process [15]. At high pH, Fe^{2+} ions from the iron surface and hydroxyl ions in the alkaline solution reacted to precipitate ferrous hydroxide on the surface of the iron occupying the reactive sites, thus hindering the reaction. Therefore, by raising pH to the alkaline region Shu et al. observed lower decolorization rates under NZVI reduction conditions. On the other hand, at acidic pH of 2, the NZVI dissolved

quickly into the bulk solution, resulting in an insufficient amount of surface area for the release of ferrous ions and electrons that degrade dye [15]. The effect of pH on decolorization of RB5 by nFeNi-GAC is illustrated in Fig. 7(a) with initial dye concentration of 50 mg l^{-1} and nFeNi-GAC dosage of 20 g l^{-1} . Elevating the pH to 12 by addition of sodium hydroxide solution (1.0 mol l^{-1}) resulted in insignificant change in RB5 degradation efficiency, whereas, reducing the pH to 2 by addition of hydrochloric acid (1.0 mol l^{-1}) resulted in slight better RB5 decolorization than pH 3–9. This implies that GAC with extreme specific surface area can protect nano iron-nickel bimetallic particles in the nFeNi-GAC surface to oxidize or corrosive dissolve as well as lose its reductive reactivity. To verify this shield effect of GAC, reductive decolorization experiments were performed for RB5 by Fe-Ni bimetallic nanoparticles without GAC support at various pH conditions. The results in Fig. 7(b) demonstrate that at extreme pH levels such as 2 and 12 inhibit decolorization of RB5 for different reasons. For an alkaline pH of 12, the precipitation of ferrous hydroxide on the surface of the Fe-Ni bimetallic nanoparticles occupying the reactive sites stopped the release of ferrous ions and electrons that cause the lowering of the reaction rate. At acidic pH of 2, the Fe-Ni bimetallic nanoparticles dissolved fast into solution. Thus, the

loss of Fe-Ni bimetallic nanoparticles results in insufficient surface area for the release of ferrous ions and electrons which react with RB5. For middle pH levels from 3 to 9, decolorization of RB5 was performed fairly efficiently with no significant differences. It is an important outcome that the GAC supporting material can be a good protecting shield for Fe-Ni bimetallic nanoparticles in nFeNi-GAC to ensure the effectiveness for various pH operating conditions.

3.5. Effect of reaction temperature

Since the effluents from dyeing industries always contain high temperature, it is important to investigate the temperature effect on reductive degradation of RB5 by nFeNi-GAC. To perform this set of experiments. A temperature control system was used to adjust the reaction temperature through a water jacket surround the reactor vessel. The reaction occurs in water/nFeNi-GAC interphase, this limits phase transfer, making it difficult to reach 100% degradation efficiency. However, increased temperature can enhance the reaction rate through kinetic fundamentals. Fig. 8 presents the effect of temperature on RB5 reductive degradation. The results show that the RB5 decolorization was affected by temperature control significantly.

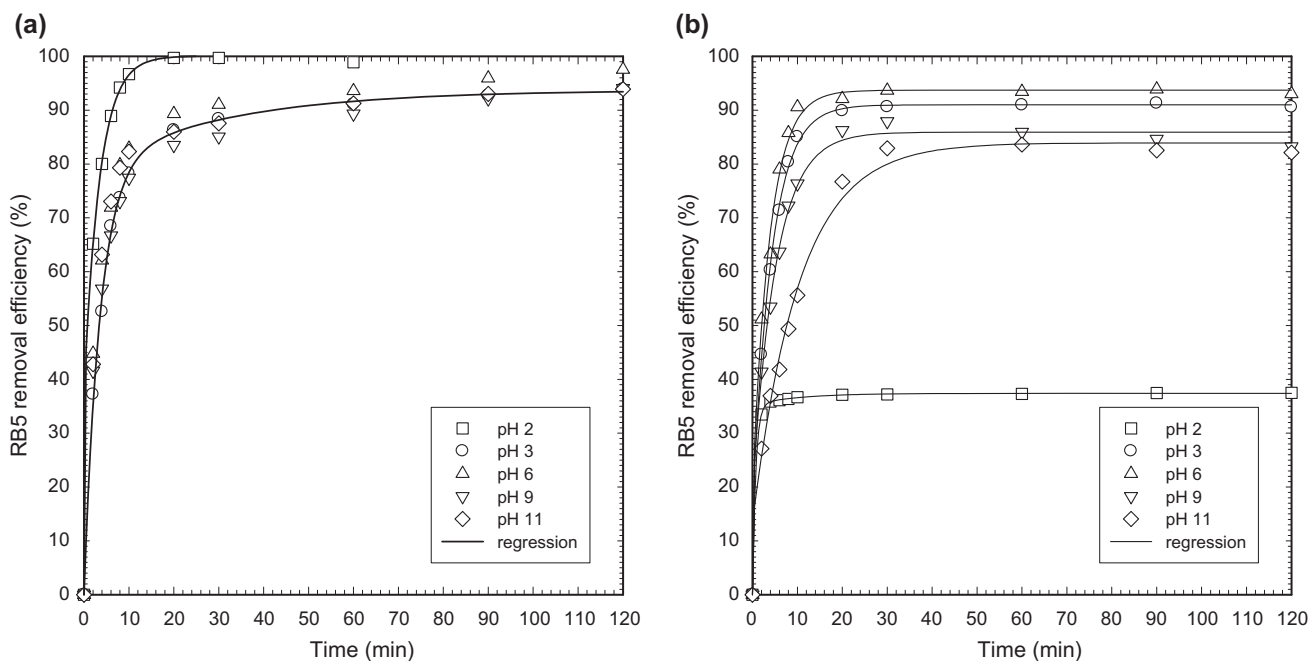


Fig. 7. Effect of initial pH on RB5 degradation by (a) nFeNi-GAC and (b) Fe-Ni bimetallic nanoparticles. The conditions were initial dye concentration of 50 mg l^{-1} , Fe/Ni load on nFeNi-GAC of $6.91 \text{ mg Fe}/0.86 \text{ mg Ni g}^{-1}$, nFeNi-GAC dosage of 20 g l^{-1} and reaction time during 120 min (Fe-Ni bimetallic nanoparticles dosage $90 \text{ mg Fe}/40 \text{ mg Ni l}^{-1}$).

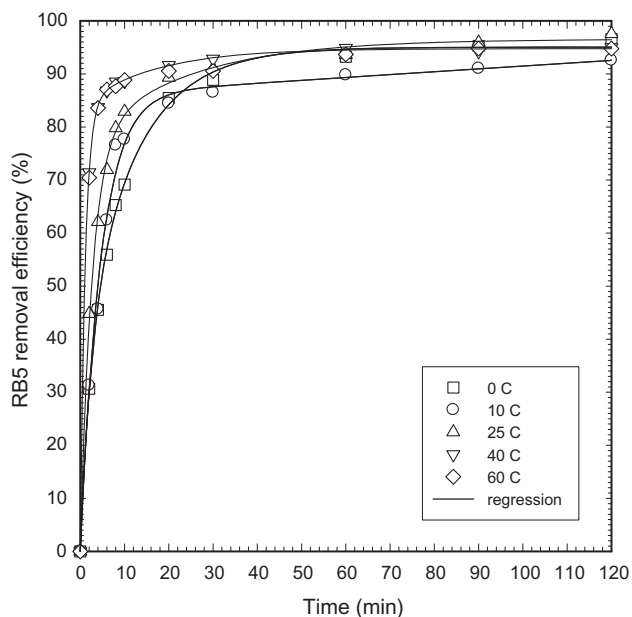


Fig. 8. Effect of reaction temperature on RB5 degradation under nFeNi-GAC process. The conditions were initial dye concentration of 50 mg l^{-1} , Fe/Ni load on nFeNi-GAC of $6.91 \text{ mg Fe}/0.86 \text{ mg Ni g}^{-1}$, nFeNi-GAC dosage of 20 g l^{-1} , and reaction time during 120 min.

The higher RB5 removal efficiencies can be reached by operating under higher temperature such as 60°C . However, for longer reaction time of 120 min the removal efficiencies for all operating temperatures reached 90–97%.

3.6. The durability test

The nFeNi-GAC material was used repeatedly to treat the RB5 solution. Fig. 9(a) shows the system performance over three cycles. Results indicated that although the rate of RB5 degradation decreased as the reuse cycle of nFeNi-GAC increased to three, the total amount of dye removal remained relatively unchanged at 95% in the treatment time range of 120 min, however. The reason for decay in reductive degradation ability is due to the oxidation of nano Fe/Ni bimetallic particles on nFeNi-GAC which inhibits the dissolution of iron and electrons. The evidence can be observed in Fig. 9(b), as ORP changes during three reuse cycles. For fresh used nFeNi-GAC, the ORP can decrease down to -620 mV . However, when used for the first and second reuse cycles, the ORP were down to about -400 and -220 mV , respectively. The results show the loss of reductive reactivity of nFeNi-GAC material by reuse cycles.

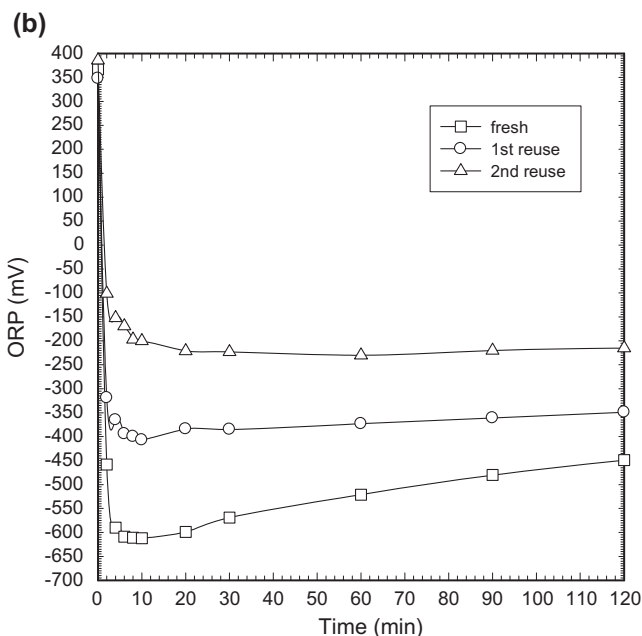
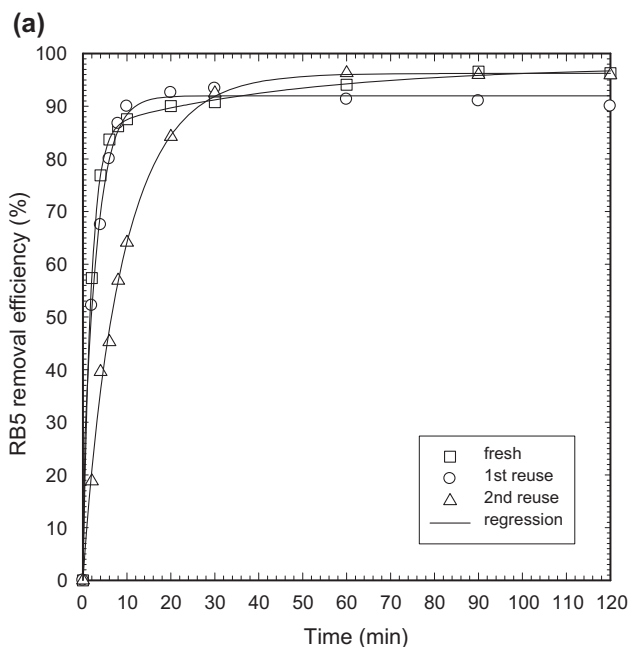


Fig. 9. (a) Effect of durability on RB5 degradation under nFeNi-GAC process. (b) The ORP changes during the reductive degradation reaction for three operation cycles. The conditions were initial dye concentration of 50 mg l^{-1} , Fe/Ni load on nFeNi-GAC of $6.91 \text{ mg Fe}/0.86 \text{ mg Ni g}^{-1}$, nFeNi-GAC dosage of 20 g l^{-1} , and reaction time during 120 min.

4. Conclusions

We have shown that reductive degradation of Reactive Black 5 di-azo dye in aqueous solution can be achieved in less than 20 min by adding activated carbon supported nano iron-nickel bimetallic complex material, namely nFeNi-GAC, under ambient conditions without pH control. After 120 min, more than 97.6% RB5 concentration and 98.9% ADMI removal were reached with a 6.91 mg Fe/0.86 mg Ni g⁻¹ load, 20 g l⁻¹ nFeNi-GAC, and initial dye solution of 50 mg l⁻¹. In our batch test, the RB5 removal efficiency was dominated by the nFeNi-GAC load as well as the initial dye concentration pH and temperature. Furthermore, the degradation efficiency increased with increased nFeNi-GAC load. An important finding of this alternative nFeNi-GAC complex material is that it provides good protecting shield for Fe-Ni bimetallic nanoparticles on GAC supporter to resist extreme pH condition such as pH 2 and 11 to ensure the color removal effectiveness. Accordingly, the results of this study on the effects of nFeNi-GAC loads, initial dye concentration and pH can optimize the operating parameters of RB5 degradation and provide industries with useful information about this alternative wastewater technology.

Acknowledgments

The authors appreciate the research funding granted by the Taiwan National Science Foundation (NSC 101-2221-E-241-004-MY3).

References

- [1] Taiwan Ministry of Finance, Brief Export–Import Statistics Monthly (Air Mail Edition)/Summary Explanation for December 2012 (Department of Statistics—2012/12/23). Available from: <http://www.mof.gov.tw/engweb/ct.asp?xItem=28631&CtNode=683&mp=2> (accessed 15 January 2014).
- [2] U. Kalsoom, S.S. Ashraf, M.A. Meetani, M.A. Rauf, H.N. Bhatti, Degradation and kinetics of H₂O₂ assisted photochemical oxidation of Remazol Turquoise Blue, *Chem. Eng. J.* 200–202 (2012) 373–379.
- [3] M.E. Nagel-Hassemer, C.R.S. Carvalho-Pinto, W.G. Matias, F.R. Lapolli, Removal of coloured compounds from textile industry effluents by UV/H₂O₂ advanced oxidation and toxicity evaluation, *Environ. Technol.* 32 (2011) 1867–1874.
- [4] X. Xu, X. Li, Degradation of azo dye Orange G in aqueous solutions by persulfate with ferrous ion, *Sep. Purif. Technol.* 72 (2010) 105–111.
- [5] H.Y. Shu, M.C. Chang, Decolorization effects of six azo dyes by O₃, UV/O₃ and UV/H₂O₂ processes, *Dyes Pigm.* 65 (2005) 25–31.
- [6] M.C. Chang, C.P. Huang, H.Y. Shu, Y.C. Chang, A new photocatalytic system using steel mesh and cold cathode fluorescent light for the decolorization of azo dye orange G, *Int. J. Photoenergy* 2012 (2012) 1–9.
- [7] T. Kim, C. Park, J. Yang, S. Kim, Comparison of disperse and reactive dye removals by chemical coagulation and Fenton oxidation, *J. Hazard. Mater.* 112 (2004) 95–103.
- [8] Y. Liu, G.V. Lowry, Effect of particle age (FeO content) and solution pH on NZVI reactivity: H₂ evolution and TCE dechlorination, *Environ. Sci. Technol.* 40 (2006) 6085–6090.
- [9] G.V. Lowry, K.M. Johnson, Congener-specific dechlorination of dissolved PCBs by microscale and nanoscale zerovalent iron in a water/methanol solution, *Environ. Sci. Technol.* 38 (2004) 5208–5216.
- [10] H. Lien, W.X. Zhang, Hydrodechlorination of chlorinated ethanes by nanoscale Pd/Fe bimetallic particles, *J. Environ. Eng.* 131 (2005) 4–10.
- [11] Z. Xiong, D. Zhao, G. Pan, Rapid and controlled transformation of nitrate in water and brine by stabilized iron nanoparticles, *J. Nanopart. Res.* 11 (2009) 807–819.
- [12] Z. Xiong, D. Zhao, G. Pan, Rapid and complete destruction of perchlorate in water and ion-exchange brine using stabilized zero-valent iron nanoparticles, *Water Res.* 41 (2007) 3497–3505.
- [13] Ç. Üzümlü, T. Shahwan, A.E. Eroglu, K.R. Hallam, T.B. Scott, I. Lieberwirth, Synthesis and characterization of kaolinite-supported zero-valent iron nanoparticles and their application for the removal of aqueous Cu²⁺ and Co²⁺ ions, *Appl. Clay Sci.* 43 (2009) 172–181.
- [14] M.C. Chang, H.Y. Shu, H.H. Yu, Y.C. Sung, Reductive decolorization and total organic carbon reduction of the diazo dye CI Acid Black 24 by zero-valent iron powder, *J. Chem. Technol. Biotechnol.* 81 (2006) 1259–1266.
- [15] H.Y. Shu, M.C. Chang, H.H. Yu, W.H. Chen, Reduction of an azo dye Acid Black 24 solution using synthesized nanoscale zerovalent iron particles, *J. Colloid Interface Sci.* 314 (2007) 89–97.
- [16] A. Li, C. Tai, Z. Zhao, Y. Wang, Q. Zhang, G. Jiang, J. Hu, Debromination of decabrominated diphenyl ether by resin-bound iron nanoparticles, *Environ. Sci. Technol.* 41 (2007) 6841–6846.
- [17] H.Y. Shu, M.C. Chang, C.C. Chen, P.E. Chen, Using resin supported nano zero-valent iron particles for decoloration of Acid Blue 113 azo dye solution, *J. Hazard. Mater.* 184 (2010) 499–505.